Electronic Supplementary Information

Tunable T_1 and T_2 contrast abilities of manganese-engineered iron oxide nanoparticles through size control

Guoming Huang,[a] Hui Li,[b] Jiahe Chen,[c] Zhenghuan Zhao,[a] Lijiao Yang,[a] Xiaoqin Chi,[b] Zhong Chen,[c] Xiaomin Wang[b] and Jinhao Gao*[a]

[a] *State Key Laboratory of Physical Chemistry of Solid Surfaces, The Key Laboratory for Chemical Biology of Fujian Province and Department of Chemical Biology, Colloge of Chemistry and Chemical Engineering, Xiamen University, Xiamen 361005, China.*

[b] *Fujian Provincial Key Laboratory of Chronic Liver Disease and Hepatocellular Carcinoma, Zhongshan Hospital, Xiamen University, Xiamen 361004, China.*

[c] *Department of Electronic Science, Fujian Key Laboratory of Plasma and Magnetic Resonance, Xiamen University, Xiamen 361005, China*

*Email: *jhgao@xmu.edu.cn*

Table S1. Size distributions and Fe/Mn molar ratios of the MnIO nanoparticles. Size distributions were obtained from TEM and XRD analysis, respectively. Fe/Mn ratios of the samples were determined by ICP-AES.

Sample	TEM size (nm)	XRD size (nm)	Fe/Mn
5 nm	5.06 ± 0.52	5.51	5.18 ± 0.11
7 nm	7.04 ± 0.58	7.30	5.03 ± 0.20
9 nm	8.98 ± 0.81	9.25	5.36 ± 0.31
12 nm	12.20 ± 0.86	11.64	5.39 ± 0.37

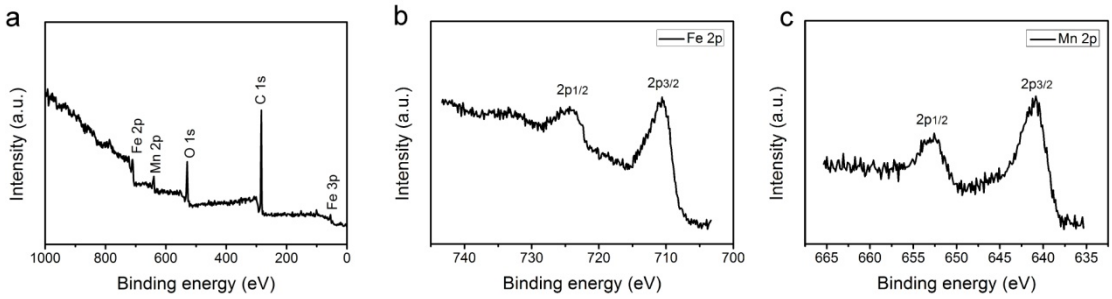

Figure S1. (a) Survey X-ray photoelectron spectroscopy (XPS) spectrum, (b) Fe 2p spectrum, and (c) Mn 2p spectrum of 12 nm MnIO nanoparticles.

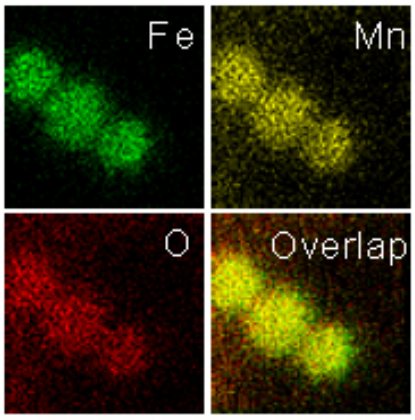

Figure S2. Energy-dispersive X-ray (EDX) mapping images of 12 nm MnIO nanoparticles.

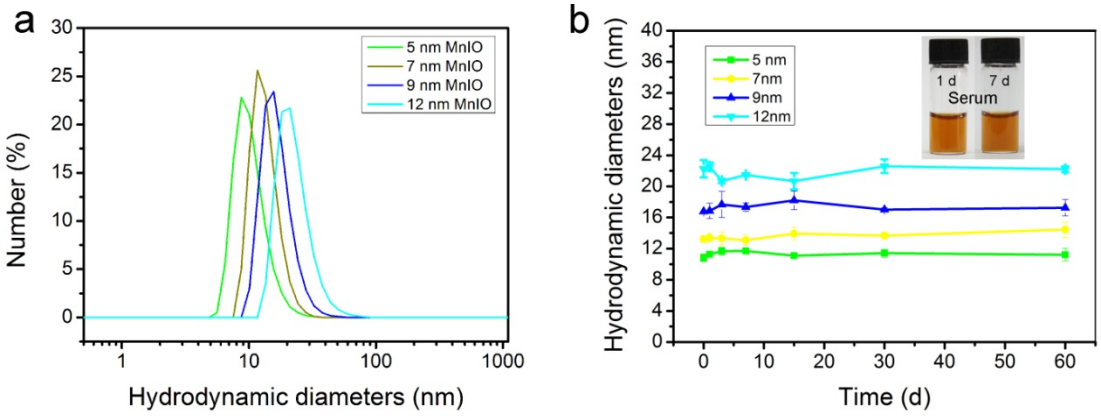

Figure S3. (a) Hydrodynamic diameter (HD) analysis and (b) HD distribution over 60 days of 5 nm, 7 nm, 9 nm, and 12 nm MnIO nanoparticles in water. Inset: photos of 12 nm MnIO nanoparticles dispersed in 10% fetal bovine serum (FBS). The solution is stable without aggregation over 7 days.

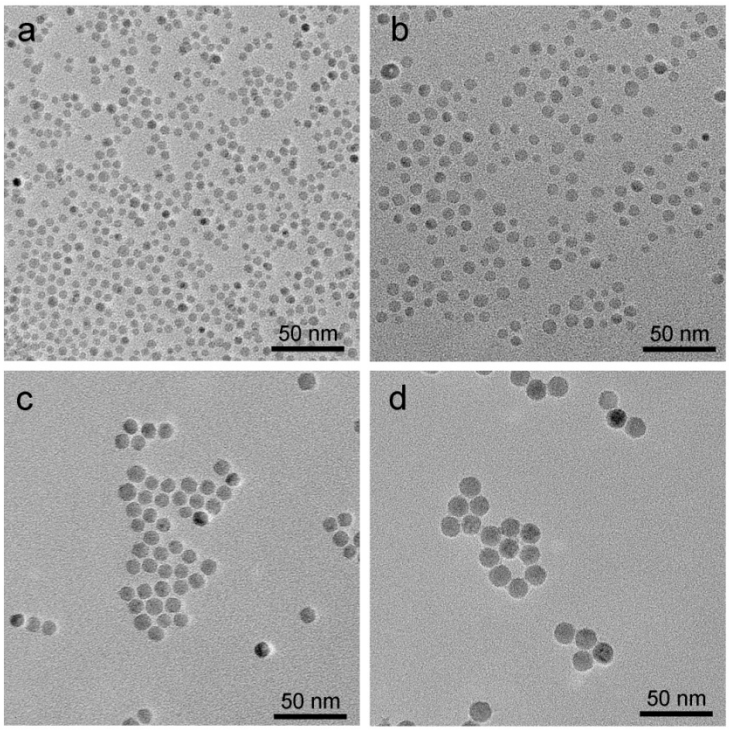

Figure S4. TEM images of (a) 5 nm, (b) 7 nm, (c) 9 nm, and (d) 12 nm MnIO nanoparticles dispersed in aqueous solution, respectively.

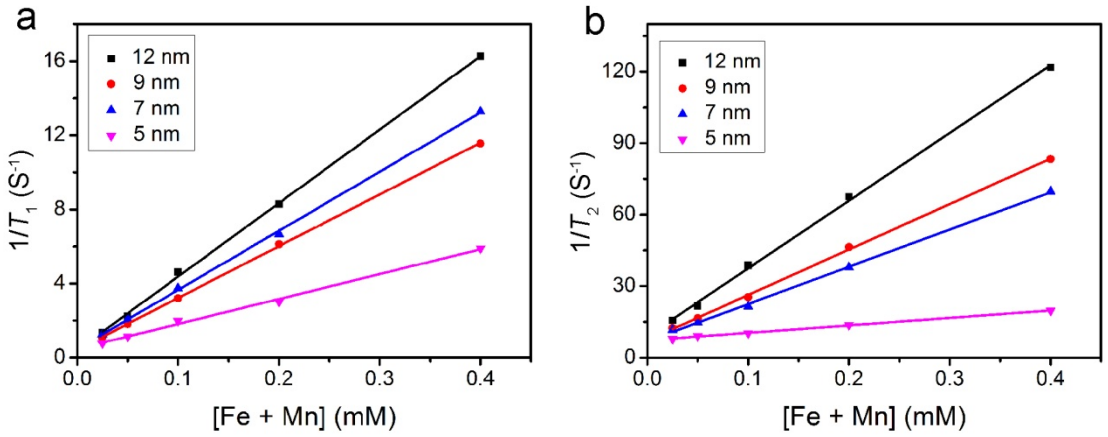

Figure S5. The linear fitting of (a) longitudinal and (b) transverse relaxation rates at 0.5 T versus magnetic metal (Fe + Mn) concentrations for 12 nm, 9 nm, 7 nm, and 5 nm MnIO nanoparticles.

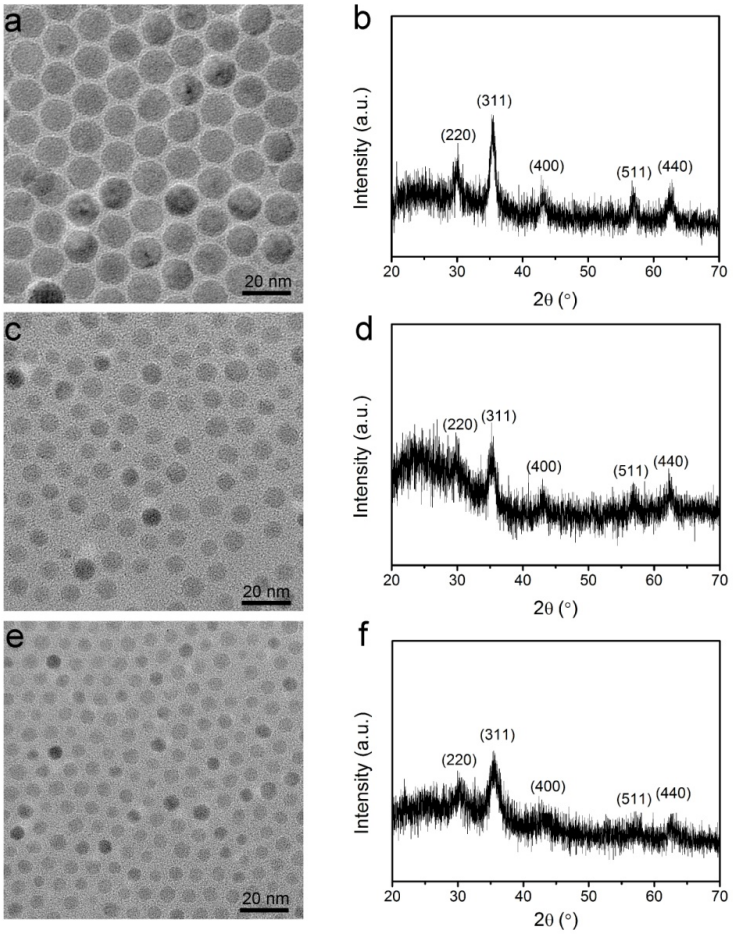

Figure S6. TEM images and XRD patterns of (a, b) 12 nm, (c, d) 7 nm, and (e, f) 5 nm IO nanoparticles, respectively.

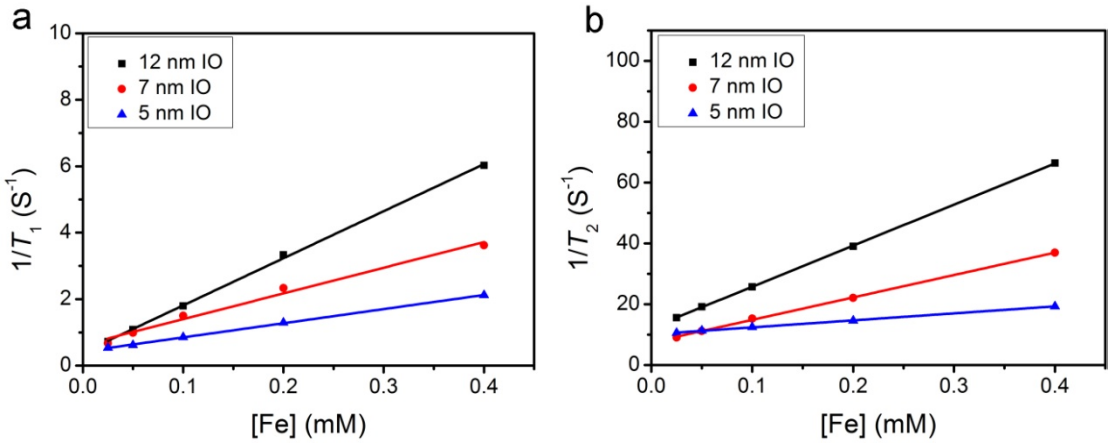

Figure S7. The linear fitting of (a) longitudinal and (b) transverse relaxation rates at 0.5 T versus Fe concentrations for 12 nm, 7 nm, and 5 nm IO nanoparticles.

Table S2. Summary of r_1, r_2, and r_2/r_1 ratios for 12 nm, 7 nm, and 5 nm IO nanoparticles at 0.5 T.

IO	r_2 ($mM^{-1}s^{-1}$)	r_1 ($mM^{-1}s^{-1}$)	r_2/r_1
12 nm	135.2	14.2	9.5
7 nm	73.7	7.7	9.6
5 nm	23.0	4.3	5.3

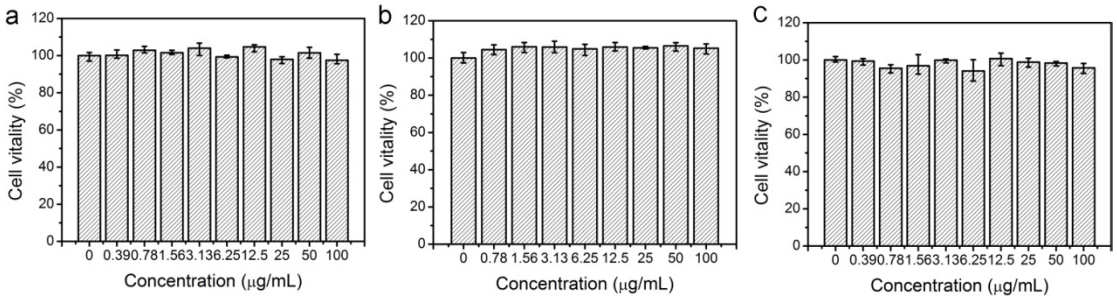

Figure S8. Cell viability of HeLa cells after incubated with (a) 12 nm, (b) 7 nm and (c) 5 nm MnIO nanoparticles with different metal ion (Fe + Mn) concentrations at 37 °C for 24 h, respectively.

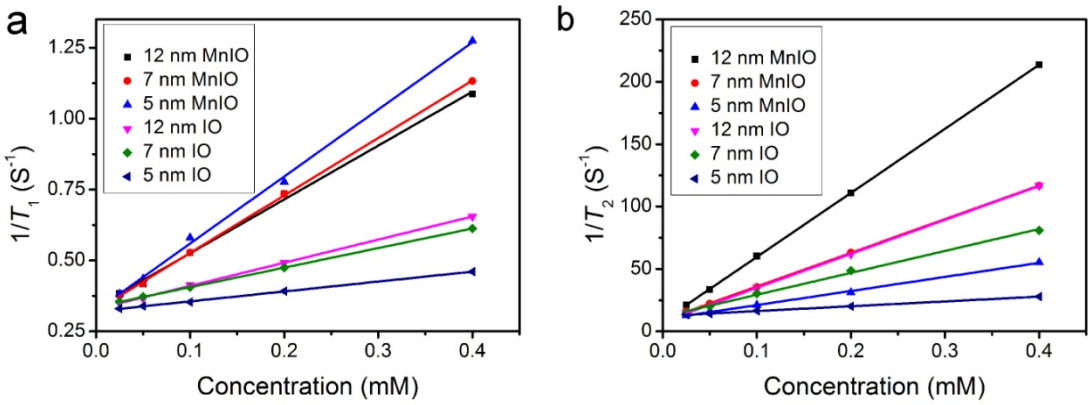

Figure S9. The linear fitting of (a) longitudinal and (b) transverse relaxation rates at 7 T versus metal ion ([Fe + Mn] for MnIO, [Fe] for IO) concentrations for 12 nm, 7 nm, and 5 nm MnIO or IO nanoparticles.

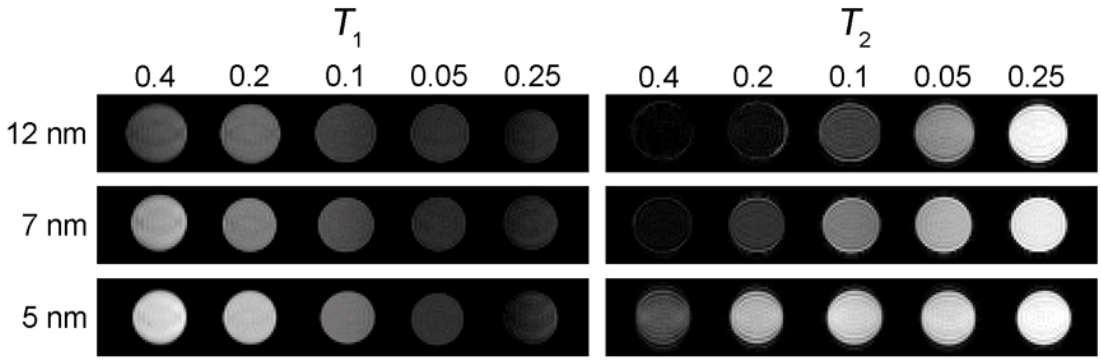

Figure S10. T_1- and T_2-weighted phantom images of 5 nm, 7 nm, and 12 nm MnIO nanoparticles in aqueous solution (containing 1% agar) with different metal ion (Fe + Mn, mM) concentrations at 7 T.

Table S3. Summary of r_1, r_2, and r_2 / r_1 ratios for 12 nm, 7 nm, and 5 nm MnIO or IO nanoparticles at 7 T.

Sizes	MnIO			IO		
	r_2 ($mM^{-1}s^{-1}$)	r_1 ($mM^{-1}s^{-1}$)	r_2/r_1	r_2 ($mM^{-1}s^{-1}$)	r_1 ($mM^{-1}s^{-1}$)	r_2/r_1
12 nm	513.37	1.90	270.19	272.04	0.82	331.76
7 nm	269.90	2.03	132.96	175.53	0.69	254.39
5 nm	112.79	2.37	47.59	38.88	0.35	111.08

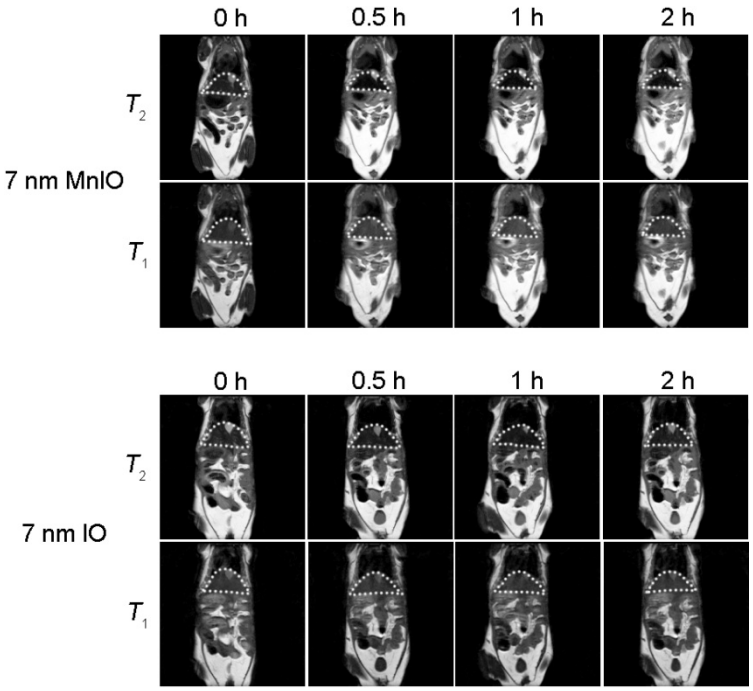

Figure S11. T_1- and T_2-weighted *in vivo* MRI images of mice (coronal plane) collected at different time points after intravenous injection of 7 nm MnIO nanoparticles and IO nanoparticles (with a dose of 2.0 mg [Fe + Mn] or [Fe] per kg of mouse body weight). The T_1- and T_2-weighted images were acquired sequentially in the same mouse. The regions of liver were indicated by dash lines.